

## Comparison of Long-term variability of Sea Surface Temperature in the Arabian Sea and Bay of Bengal

P. K. Dinesh Kumar<sup>a\*</sup>, Y. Steeven Paul<sup>b</sup>, K.R. Muraleedharan<sup>a</sup>, V.S.N. Murty<sup>b</sup> and P.N. Preenu<sup>a</sup>

<sup>a</sup>Council of Scientific and Industrial Research (CSIR) – National Institute of Oceanography, Regional Centre, Dr.Salim Ali Road, Kochi – 682 018, Kerala, India

<sup>b</sup>Council of Scientific and Industrial Research (CSIR) – National Institute of Oceanography, Regional Centre, Visakhapatnam – 530017, India

\*Corresponding Author: email: [dineshku@nio.org](mailto:dineshku@nio.org); phone:+91 484 2390 814; fax: +91 484 2390618

### Abstract

Long-term variability of Sea Surface Temperature (SST) in the Arabian Sea (AS) and Bay of Bengal (BoB) during 1880-2010 is examined using all the available data sets of monthly SST, wind speed, incoming solar radiation, cloud cover, long wave radiation, latent heat flux, net surface heat flux and surface currents. SST time series reveal an upward (increasing) trend (warming) after 1940 in both the basins. Wavelet analyses of the SST time series reveal that AS SST is controlled by semi-annual and annual forcing while the BoB SST is influenced predominantly by annual forcing. The SST responses in both the basins are in phase to the climatic events such as El Niño, La Niña and Indian Ocean Dipole, but a stronger impact is noticed in the AS SST. The climatic events affected the seasonal peaks of SST warming (April-May) and cooling (August-September) in both the basins. Time series of SST anomaly also showed in phase responses to the climatic events and an upward trend from 1960 to 2010 in both the basins. Long-term decreasing trends observed in surface wind speed, latent heat flux and advective process *via* the weakened surface currents, together with the long-term increasing trend in P-E (Precipitation, P minus Evaporation, E) contributed to the SST warming trend in both the basins. In association with the upward trend in P-E, the Simple Ocean Data Assimilation (SODA) Reanalysis Sea Surface Salinity time series exhibited freshening (a decreasing trend) and enhanced the salinity stratification in the BoB, thus modulated the BoB SST warming. These cumulative processes led to the warmer SSTs in the BoB compared to that in AS.

**Key words:** sea surface temperature; Arabian Sea; Bay of Bengal; India; climate change

## 1. Introduction

The northern Indian Ocean basin is entirely different from other world oceans due to its confinement within the tropics and lack of connection to the northern polar region. The Indian peninsula divides the north Indian Ocean into two basins - the AS and the BoB which experience the semi-annually reversing southwest (SW) and northeast (NE) monsoonal winds. Accordingly, the wind driven surface circulation in both the basins undergoes seasonal reversal (Dietrich 1973; Murty et al., 1992; Conkright et al., 1994; Varkey et al., 1996; Shankar et al., 2002). The current systems in the northern Indian Ocean is characterised by the seasonally changing monsoon gyre. The circulation is stronger and steadier during the SW monsoon than during NE monsoon which has no parallel in other oceans.

The Sea Surface Temperature (SST) is a direct measure of the energy balance which drives the circulation and ultimately defines the climate. The energy transferred between the ocean and the atmosphere is to a large extent dependent on SST and functions of SST such as the sensible heat flux, latent heat flux, and radiative flux at the sea surface. SST is an important physical property of the ocean to understand the features like current flows, precipitation, biological production, properties of surface air over the ocean, upwelling etc. SST is influenced by the parameters such as net incoming shortwave solar radiation, net long wave radiation, and the turbulent air-sea heat fluxes (the latent heat and sensible heat fluxes), wind stress curl, mixed layer depth, advection of eddies and ocean currents (Rao et al., 1994; Wilson-Diaz et al., 2009).

In both the AS and BoB, the annual variation of SST exhibits bi-modal character (Colborn, 1975) exhibiting surface warming in April-May and October and surface cooling during SW monsoon and winter months. However, the AS cools more during SW monsoon than does the BoB. Earlier studies suggested that the AS SST is important because of its possible role in the inter-annual variability of Indian summer monsoon (Li et al., 2001; Vinayachandran, 2004; Wilson Diaz et al., 2009). Ellis (1952) showed that the floods of 1920 and the droughts of 1933 over a large area of the Indian sub-continent were well correlated with the AS SST anomalies. The AS SST exhibits a distinct spatial gradient, with lower SST in the west compared to that in the east (Rao, 1988) during the southwest monsoon. During April – May, the north Indian Ocean becomes the warmest area among the world oceans (Joseph, 1990). Soon after the onset of monsoon in June the surface winds strengthen, latent heat flux increases, SST decreases and the AS cools rapidly (Shenoi et al., 2002), though this cooling is not uniform in all parts of the AS (Ramesh Babu and Sastry, 1984). In the BoB, the lesser SST cooling is due to the heavy

precipitation and fresh water runoff and the associated near-surface stratification during the SW monsoon (Shenoi et al., 2002).

The AS SST has a large influence on the wind patterns over India (Shukla and Misra, 1977; Ramesh Babu and Sastry, 1984; Vinayachandran, 2004) and on the Indian monsoon rain fall (Prasanna Kumar et al., 2009). Winds are strong over the AS due to the presence of Findlater Jet (Shenoi et al., 2002) compared to that over the BoB during the SW monsoon. Stronger winds cause increase in evaporation, upwelling and spreading of coastal cold waters off Arabia and Somalia coasts, resulting in wide spread of colder SST waters into the central AS. Onset of monsoon (Vinayachandran, 2004) and the biological production (Murtugudde et al., 2007) in the AS are closely related to the SST. The heat transfer between the atmosphere and ocean is dependent upon SST. Joseph (1990) studied the relation of warm pool and onset of summer monsoon, while Rao and Sivakumar (1999) studied the variation in SST. A mini-warm pool with higher SST ( $\sim 31^{\circ}\text{C}$ ) occurs in the south-eastern Arabian Sea prior to the onset of SW monsoon (Vinayachandran et al., 2007; Ebenezer et al., 2012). Molinari et al. (1986) reported that much of the SST variability in the AS can be predicted by the surface fluxes alone but in coastal areas the horizontal advection of heat and entrainment of subsurface water are to be considered.

The BoB receives more extensive fresh water from precipitation and river run off than the AS (Varkey et al., 1996; Shenoi et al., 2002) and hence the former is less saline. Saji et al. (1999) have pointed out that Indian Ocean give birth to a unique coupled ocean-atmosphere mode categorized as the manifestation of the tropical air-sea interaction. A shift in SST was reported in the Indian Ocean after 1976-77 (Terray, 1994; Terray and Dominiak, 2005) and a clear shift of SST in the AS after 1995 (Prasanna Kumar et al., 2009).

Long-term perspective of variations in SST in the AS and BoB and their comparison are required for a range of purposes. This knowledge would help in assessing whether the future climate scenario shows a continuation of recent variability or shows extreme case. It would also be required to overcome the inherent variability of climate models. In this direction, in the present study we have attempted to compare the long-term variability in SST in the AS and BoB using the long-term data records over a period of 130 years from 1880 to 2010. The goal of this study is to gain some insight into the processes controlling the forcing by utilizing all the available gridded data sets and raise questions about the climate change in response to natural and anthropogenic sources. Primarily using the ERSST, this study details the SST/SST anomalies from 1880 to 2010 for the Arabian Sea (AS) and Bay of Bengal (BoB) and using various heat flux components the mechanisms causing the SST variability are brought out.

The paper is organized as follows: Section 2 describes various datasets and methods used. Detailed analyses of long-term variability in SST and SST anomaly in the AS and the BoB are presented in section 3.1. In section 3.2 we investigate the linkages between the SST anomaly variability in the AS and BoB and the climatic events such as the Indian Ocean Dipole (IOD), El Niño and La Niña. Section 3.3 deals with the long-term variation of the air-sea interaction parameters and surface currents in the AS and BoB. A summary and discussion of our findings are presented in section 4.

## 2. Materials and Methods

For the present study, the region between 10°-20°N and 60°-70°E in the AS and the region between 10°-20°N and 85°-95°E in BoB are considered (Fig. 1). Monthly mean SST data was extracted from the NOAA extended reconstructed monthly Sea Surface Temperature (ERSST), version 3, from 1880 to 2010 (<http://www.esrl.noaa.gov/psd/data/gridded/data.noaa.ersst.html>). This ERSST product contains the SST estimates from satellites, ships and buoys merged using a weighted sum of the different inputs, with weights inversely proportional to the noise estimate for each type (Smith et al., 2008). The monthly analysis extends from January 1854 to the present, but because of sparse data in the early years, the analysed signal is weak before 1880. After 1880, the strength of the signal is more consistent over time (Ihara et al., 2008). Hence, the data were selected from 1880 to 2009. ERSST is suitable for long-term global and basin wide studies; local and short-term variations have been smoothed in ERSST. By fitting to a set of spatial modes, the high-frequency SST anomalies have been reconstructed. For checking the quality of the data set, the ERSST data is compared with the Conkright et al. (1994) monthly temperature data.

Parameters such as SST, wind speed, shortwave radiation, long wave radiation, latent heat flux, and cloud cover were analysed using the monthly data from National Centre for Environment Prediction (NCEP)/National Centre and Atmospheric Research (NCAR) reanalysis 1 product for the period from 1948 to 2011 with 2.5° × 2.5° resolution. The recently developed new global Tropical air-sea heat Fluxes (TropFlux) data products (Praveen Kumar et al., 2012a) on improved air-sea heat fluxes, reconstructed solar radiation and evaporation were also analysed. The Objectively Analysed air-sea heat Fluxes (OAFlux) data products (Yu and Weller, 2007) developed at Woods Hole Oceanographic Institute (WHOI) on sensible and latent heat fluxes, which were validated by using *in situ* flux measurements, were analysed for the period from 1958 to 2010. The Hadley Sea Surface Temperature (HadISST1) product at 1°x1° grids (Rayner et al., 2003) developed at the Met Office Hadley Centre, UK, for the period 1880-2008 (<http://www.metoffice.gov.uk/hadobs/hadisst/>) was also analysed in conjunction with

that of ERSST SST product of the same period. Simple Ocean Data Assimilation (SODA) Reanalysis data product (Carton and Giese, 2008) on near-surface temperature (taken as SST) were also analysed for the period 1940-2008. Ocean current data from 1965 to 2005 were downloaded from Geophysical Fluid Dynamic Laboratory (<http://www.gfdl.noaa.gov/ocean-data-assimilation/>).

The above mentioned long-term data sets were subjected to trend analysis for both the AS and BoB boxes (Fig. 1). To examine the seasonal and inter-annual variations in the data set, two year smoothing was done and anomalies were calculated. Wavelet analysis was carried out to examine the dominant factors that would bring variability in the SST at seasonal and inter-annual time scales. Wavelet spectra were based on Morlet wavelets calculated as described in Torrence and Compo (1998). The advantage of wavelet transform over traditional Fast Fourier Transform (FFT) analysis is that it provides clearer variation of structures with time and space than FFT analysis does (Shankar et al., 2010). At inter-annual time scale, the climatic events such as the Indian Ocean Dipole (IOD), El Niño and La Niña bring in the SST variability. Table 1 provides the information on the occurrences of the climatic events of IOD, El Niño and La Niña either independently or co-occurring with the other events during 1960-2008 (Nyadjro et al., 2013).

### 3. Results

Patterns of SST variability on longer time scales result from a combination of numerous processes. The climate of the basins is controlled by large pressure systems that govern the wind field over the continent and oceans. The prevalent SST patterns are due to the resultant modes of different time scales of air-sea interaction processes that affect the SST field. Hence, analyses of long term data sets of SST, SST anomalies, surface wind speed, short and long wave radiation, air-sea heat fluxes (latent heat), evaporation, and sea surface currents were carried out.

#### *3.1 Long-term variation of SST in the AS and BoB*

Time series of ERSST in the AS and BoB for the period 1880-2009 are shown in Fig. 2. One can notice warmer SSTs in the BoB compared to the AS, however, the maximum and minimum SST in both the basins are in phase suggesting that both the basins responded equally to the IOD, El Niño and La Niña climatic events. Minimum surface temperature occurred during 1893 and the maximum during 1942-44. Larger response is seen in the AS compared to that in the BoB. This long term SST variation suggests the occurrence of decadal variability in both the basins.

Warming trend in SST could be seen in both the AS and BoB during the period 1940–2009. The rate of SST warming is about  $0.075^{\circ}\text{C}/\text{decade}$  for AS and  $0.07^{\circ}\text{C}/\text{decade}$  for BoB during this period. The SST trend for the period 1900-1950 is, however, very weak ( $0.008^{\circ}\text{C}/\text{decade}$  in the AS and  $0.04^{\circ}\text{C}/\text{decade}$  in the BoB). For the period 1960 to 2009, the rate of SST increase is almost uniform at  $0.12^{\circ}\text{C}/\text{decade}$  in both AS and BoB.

Though the wavelet spectra carried out to the ERSST time series SST data for AS (Fig. 3) and BoB (Fig. 4) yielded significant power peaks at both the semi-annual and annual periods, the annual process appeared to be more significant and predominant in the BoB.

A comparison of mean seasonal cycles of ERSST SST over the period 1880-2009 in the AS and BoB (Fig. 5) identifies the clearer bimodal variation (Colborn 1975) with predominantly higher SST during the spring-intermonsoon warming season (March-May) with a peak value of SST in April. Both the basins attain equal maximum SST in the month of April, and a secondary warming peak in September-October. In both the basins, a large difference in SST is noticed in July with relatively colder SST in the AS and a weaker SST cooling in the BoB. The seasonal cycle of SST in the BoB registers higher temperatures and large differences in SST during the SW monsoon (June-September). The seasonal cycles of SST clearly suggest that warming in AS is strongly influenced by the spring-intermonsoon primary warming (March-May) and fall-intermonsoon secondary warming (September-October) and inter-annual processes. The SSTs in AS and BoB exhibit warmer temperatures during both the spring- and fall-intermonsoons. In the BoB, the spectral energy associated with the annual cycle variation is twice higher than the semi-annual cycle variability in the SST. Since the SST cooling in the BoB during the SW monsoon and the secondary SST warming during the fall-intermonsoon are relatively less, compared to those in the AS, the primary SST warming during spring-intermonsoon is responsible for the annual spectral peak dominance and the associated annual variability in the SST in the BoB.

The seasonal cycles of ERSST SST anomaly for the period 1932-1969 in the AS and BoB show similar seasonal cycle anomalies with almost constant deviation. Interestingly, weaker warmer SST anomaly of  $0.04^{\circ}$  to  $0.16^{\circ}\text{C}$  and weaker colder SST anomaly of  $-0.04^{\circ}$  to  $0.02^{\circ}\text{C}$  occurs in the AS and BoB. The seasonal cycles of SST anomaly thus obtained are opposite to those of the seasonal cycles of SST variation found in both the basins. However, the seasonal cycles of ERSST SST anomaly for the period 1970-2008 in the AS and BoB show similar seasonal variation with larger warmer anomaly ( $0.32^{\circ}$  to  $0.48^{\circ}\text{C}$ ) in both the basins with lower SST anomaly in the BoB (Fig. 6). Maximum SST anomaly is noticed during April-May and minimum SST anomaly in August. Interestingly, in both the AS and

BoB, SST anomaly increased from August to December. These seasonal cycles of SST anomaly are opposite to those of the seasonal cycles of SST variation in both the basins, and suggest that these larger SST anomalies relative to the period 1970-2008 contributed to the observed increasing trend in the SST in these basins (Fig. 2).

The long-term time series of SST anomalies derived from ERSST SST, HadISST1, SODA SST and TropFlux SST data sets are shown in fig 7 to 10. The anomalies for each data set are calculated after subtracting the seasonal cycles of SST of each data set of respective time series duration – ERSST from 1880-2009, HadISST1 from 1880-2008, SODA SST from 1940-2008 and TropFlux SST from 1979-2010.

The ERSST anomaly for the entire study period relative to the seasonal cycle for the period 1880-2009 reveals SST cooling ( $-0.2^{\circ}$  to  $-0.8^{\circ}\text{C}$ ) during 1880-1940 and warming trend during 1940-2010 with SST anomalies reaching up to  $0.8^{\circ}\text{C}$  (Fig. 7). The AS experiences relatively more cooling and warming compared to the BoB. The SST anomalies in both the basins showed an increasing trend during 1960-2009, and a little difference in SST anomalies during the past four decades (1970-2010). Relative to the seasonal cycle for the period 1971-2000, the ERSST SST anomalies reveal large SST cooling ( $-0.4^{\circ}$  to  $-1.0^{\circ}\text{C}$ ) during 1880-1960, except the period 1942-44, and for the period 1960-2009, a warming trend could be observed with values reaching up to  $0.4^{\circ}\text{C}$  (Fig. not shown). In this case also, the AS experiences higher response of cooling and warming compared to that in the BoB, and for the period 1970-2010, the response of both AS and BoB is nearly equal with smaller SST anomaly differences. It is to be noted that the upward warming trend in the SST anomalies in both the basins is unchanged with the change of mean seasonal cycle used to derive the SST anomalies, but an upward shift towards positive and warmer anomalies is noticed.

We also examined the long-term time series of HadISST1 anomaly (mean seasonal cycle removed) for the period 1880-2008 (Fig. 8). It is noticed that these Hadley SST anomaly variations are similar to those obtained using ERSST anomalies; however, the magnitude of ERSST anomaly is on the higher side in both the basins. One can see the upward increasing trend in the HadISST1 anomaly from 1965 to 2008, as that noticed in the ERSST anomaly time series. The negative and positive peaks in HadISST1 anomalies correspond to the responses of both the basins to the climatic events as mentioned in Table 1.

Examination of time series of SODA SST anomaly (mean seasonal cycle removed) for the period 1940-2008 in both the AS and BoB basins (see the identified boxes Fig. 1) reveals that these SODA SST anomaly variations are similar to those obtained using the ERSST anomalies and HadISST1 anomalies.

Here also, one can see the upward increasing trend from 1940 to 2008, as that noticed in the ERSST and HadISST1, with the negative and positive peaks corresponding to the responses of both the basins to the climatic events.

The TropFlux time series is relatively shorter (1979-2008) compared to the above long term time series. The TropFlux SST anomaly time series in the AS and BoB basins showed larger negative and positive peaks of equal magnitude. However, the long-term upward trend in SST anomalies is evident over the past 2 decades. The peaks in the SST anomalies correspond to the responses of the AS and BoB to the climatic events.

### *3.2 Linkage between the long-term SST anomalies and climatic events*

SST anomalies with positive peak ( $> 0.4^{\circ}\text{C}$ ) are found in both AS and BoB in 1942, 1963, 1968-69, 1982-83, 1987, 1997-1998, 2005 and 2008 (Figs. 7 to 10), whereas lower SST anomaly is registered in 1975, 1984 and 1988-89. These identified years of large SST anomalies correspond to the climatic events of El Niño, La Niña and IOD and their occurrence either independently or in combination (Table 1). In general, warm SST anomaly peaks are associated with positive IOD events and colder SST anomaly peaks are associated with negative IOD events. This is in agreement with the studies of Praveen Kumar (2013), who reported negative feedback between net heat flux and SST during IOD events. Similarly, warm SST anomaly peaks are associated with El Niño and colder SST anomaly peaks are associated with La Niña events, thus ENSO events (El Niño and La Niña) provide positive feedback to the SST (Praveen Kumar, 2013). In Figs. 7 to 10, a steady increase in SST anomaly is observed in both AS and BoB, with slightly lower SST anomalies in the BoB. This suggests that some amount of SST cooling occurred in the BoB during the periods of climatic events, when warming process prevailed in the AS. The observed negative (positive) SST anomalies during La Niña (El Niño) could be seen as the result of increased (decreased) net heat flux across the sea surface (Felton et al., 2013). Negative SST anomaly persisted till 1930 and afterwards a shift in the trend could be observed, except for two or three years. The negative anomalies were almost absent from 1960 in the ERSST anomaly time series, from 1975 onwards in the HadISST1 anomaly time series, from 1990 onwards in SODA SST anomaly time series, and no such demarcation in the shorter TropFlux SST anomaly time series. This suggests that one should be cautious in inferring the occurrence of climate shifts from the long term time series SST data sets. From the ERSST time series data set, a climatic shift towards warming phase could be inferred from 1965 onwards.



When the positive IOD and El Niño events co-occurred, for example in the year 1982 (Table 1), the annual variation of SST anomaly during 1981-82 was high in the AS with warm anomalies in April-May and colder anomalies in September (Fig. 11). In the BoB, the annual variation of SST anomaly shows relatively higher, warmer anomalies in November – December. As evident from the SST cooling from April to September 1982, the response of the AS to the climatic events was relatively more ( $0.1^{\circ}\text{C}$ ) than that in the BoB ( $0.065^{\circ}\text{C}$ ).

However, the responses of the AS and BoB to the independent and individual climatic events are found to be weaker ( $\sim 0.05^{\circ}\text{C}$ ) as evidenced from the annual variation of SST anomaly during 1991-1992 in these basins (Fig. 12), though the seasonal warming and cooling of SST are phase locked to April-May and September respectively. The SST anomalies are comparatively higher in the AS than in the BoB. In 1991, when only the El Niño event occurred the seasonal SST anomaly variation (April-September) is  $0.083^{\circ}\text{C}$  in both the AS and BoB. In 1992, when only a negative IOD event occurred, the seasonal SST anomaly variation is  $0.05^{\circ}\text{C}$  in the AS and  $0.06^{\circ}\text{C}$  in the BoB.

Felton et al. (2013) reported that SODA SST anomalies exhibited different patterns during El Niño and La Niña in the BoB (their Fig. 12a-b), with warmer SST anomalies prevailing in the BoB (and also in the AS) during the composite El Niño events and colder SST anomalies in the BoB (and also in the AS) during the composite La Niña events. These authors attributed this to the fact that under La Niña conditions, anomalously strong winds force evaporation that cooled the SST, while during El Niño event weaker winds and the associated weaker evaporation rate led to warmer SSTs in the BoB. Earlier, Hong et al. (2010) reported that warming or cooling during each ENSO phase in the Indian Ocean is primarily due to basin wide surface heat flux anomalies.

### *3.3 Long-term variation of the air-sea interaction parameters and sea surface currents*

In order to identify which parameter of the air-sea interaction processes has led to the observed SST anomaly variability in both the AS and BoB, we have analysed the time series of various parameters of the air-sea interaction processes. Fig. 13 shows the long-term time series of NCEP/NCAR surface wind speed in the AS and BoB during 1948-2011. Surface wind speeds over the AS and BoB exhibited a more or less similar pattern, with occasional higher wind speeds in some years. The wind speed over the AS is far higher than that over the BoB throughout the study period. During the period 1994-2011, one would see decreasing trend in the wind speed. However, the time series of wind speed difference (AS minus BoB) showed an increasing trend (Fig. not shown).

The time series of NCEP/NCAR data product on shortwave radiation (SWR,  $\text{W.m}^{-2}$ ) received at sea surface in the AS and BoB boxes during 1948 – 2008 are shown in fig.14. The AS basin receives higher SWR (200-225  $\text{W.m}^{-2}$ ) than the BoB does (185-205  $\text{W.m}^{-2}$ ). Though the time series of SWR in the AS does not show any long term trend, the SWR time series in the BoB shows increasing trend in SWR over the BoB. The SWR showed an increasing trend from 1960 to 1986 in AS and from 1962 to 2004 in BoB. After 1986 a decreasing trend was observed in AS. The minimum values of SWR in both the basins are seen during the 1957-63 period. This time series of SWR, in fact, would lead to higher SSTs in the AS and lower SSTs in the BoB, but the time series of ERSST in the AS and BoB show opposite variations.

Time series of differences in the SWR over the AS box and BoB box during 1949-2011 showed higher and lower values respectively during 1949-1983 corresponding to the impact of climatic events (Fig. 15). A decreasing trend is observed during 1994–2011 suggesting that both the basins received similar amount of SWR irrespective of whether monsoons were strong or weak in these years.

The time series of TropFlux data product on SWR received at sea surface in both the AS and BoB boxes (Fig. 1) during 1979 – 2010 reveals high SWR (210-220  $\text{W.m}^{-2}$ ) in the AS box and lower SWR (185-195  $\text{W.m}^{-2}$ ) in the BoB box (Fig. 16). Though the time series of SWR in the AS does not show any long term trend, it shows a decreasing trend in the BoB during the past two decades. This time series of SWR, in fact, would lead to higher SSTs in the AS and lower SSTs in the BoB, but the time series of ERSST in the AS and BoB show opposite variations.

The lower TropFlux SWR over the BoB box during the period 1949-2011 is due to higher cloud cover (expressed as percentage) over the BoB than AS box (Fig. 17). The long term variations in cloud cover correspond to the convection processes associated with the climatic events and the development and movement of weather systems over the BoB.

The time series of long wave radiation was high (55-69  $\text{W.m}^{-2}$ ) in the AS and low (53-61  $\text{W.m}^{-2}$ ) in the BoB box (Fig. not shown), as the moisture flux from the sea surface over the AS is higher than over the BoB. The large peaks in long wave radiation during the period 1949-2011 correspond to the impact of the climatic events.

Both the AS and BoB show large latent heat fluxes during 1949-2011 (Fig. 18). The larger latent heat over the AS contributes greatly to the heat loss from sea surface and hence leads to cooler SST. This explains the prevalent lower SSTs in the AS compared to the warmer SSTs in the BoB. Larger variations in the latent heat flux for brief periods of 1979-83, 1987-91, 1993-97 and 2002-08 in the AS

correspond to the impact of climatic events through the prevailing higher wind speeds. The variations in the latent heat flux in the BoB are relatively less during the period 1949-2011.

Long term variations in the time series of the NCEP/NCAR data product on net surface heat flux in both the AS and BoB boxes (Fig. 1) during 1948 – 2008 reveal that both AS and BoB basins experienced similar net heat flux variations with heat gain or loss at sea surface (Fig. 19). The variations of net surface heat flux show decadal oscillation in both the basins. The long-term variation indicates upward trend in the net heat flux suggesting net heat gain in both the basins, which can contribute to the long-term upward trend in the SST in both the basins.

In contrast, the TropFlux heat fluxes data during 1979-2010 showed only net heat gain at sea surface in both the AS and BoB, though the AS gains relatively higher net heat flux (Fig. 20). Occasional weaker net heat loss of  $<10 \text{ W.m}^{-2}$  occurred in 1992 and 2000. Large inter-annual variation in net heat flux is seen in both the basins. This variation of TropFlux net heat flux explains well the seasonal SST anomaly variation in both the basins, with relatively lower SST anomalies in the BoB corresponding to the lower net heat fluxes in the BoB.

It is known well that besides the air-sea interaction processes and net heat flux at the sea surface, SST variations are also controlled by the oceanic advection processes. In order to assess the impact of the advection due to surface currents in the AS and BoB boxes, we have analysed the long term variation of surface current speeds as obtained from the GFDL model simulations. Fig. 21 shows the long-term variation of surface currents in the AS and BoB boxes during 1965-2004. The surface currents (m/s) are relatively stronger in the AS than in the BoB, suggesting larger contribution of advective processes in the AS. Surface currents in the AS varied between 0.09 m/s and 0.13 m/s during 1970-72, 1979-80 and 1989-90 in the AS, and became weak after 1992 till 2004 (Fig. 21). In the BoB, the surface current speeds are very much weaker than in the AS and varied between 0.07 m/s and 0.09 m/s. The surface current speed in the BoB also decreased during the period 1992-2004. The pattern of variation in current speed in the BoB did not follow that in the AS. Difference in current speed between AS and BoB showed a decreasing trend after 1979 (Fig. not shown). The weaker surface currents in the AS and BoB during 1992-2004 would lead to weaker advective processes and contributes to the increase of SST in the presence of net surface heat gain in both the AS and BoB.

## 4. Discussion

We have examined different long-term monthly time series of ERSST, Hadley SST in  $1^{\circ} \times 1^{\circ}$  grids (HadISST1), SODA SST, OAFlux SST and TropFlux SST data products of different record lengths for the Arabian Sea box and Bay of Bengal (Fig. 1) in the northern Indian Ocean. All these data sets clearly showed an upward (increasing) trend in the SST from 1880 with relatively higher SSTs in the Bay of Bengal than in the Arabian Sea. Higher SST in the BoB compared to that in the AS was reported by Shenoi et al. (2002). The wavelet analysis of the time series SST data illustrates that the long-term SST of the AS is affected by both the semi-annual and annual forcing, while in the BoB the annual forcing appears to have more influence on the SST variation than the weaker semi-annual forcing. In order to understand the various causative factors that lead to the observed increasing trend in SST in the northern Indian Ocean, we analysed different long-term data products (NCEP/NCAR, OAFlux, TropFlux, GFDL and SODA) for various air-sea interaction parameters and oceanic parameters of surface currents and sea surface salinity (SSS). Surface winds are relatively stronger over the AS than over the BoB, and exhibited weakening trend over both the AS and BoB from 1990 onwards. This decrease of wind speed over both the basins during the past two decades impacts and lowers the latent heat flux over both the basins and thus would contribute to the observed long-term upward trend (increasing) in SST. Prasanna Kumar et al., (2009) also reported that increase in SST in the AS was followed by a decline in the intensity of wind pattern.

The long-term time series of short wave radiation and total cloud cover show that the AS receives higher solar radiation than the BoB. The time series of latent heat flux shows that the latent heat flux is relatively higher in the AS than in the BoB, but a distinct pattern of oscillation with almost similar values of latent heat flux can be seen during 1971-79 and 1991-93. Further, the latent heat flux exhibits a decreasing trend from 1995 to 2010, and thus might contribute to the increasing trend in SST in both the basins during this period. Earlier studies reported that the AS loses freshwater due to excess evaporation over precipitation, while BoB receives excess precipitation over evaporation and besides receives a huge quantity of freshwater flux from the river systems (Murty et al., 2004; Prasanna Kumar et al., 2004). The hydrological imbalance thus created on an annual scale, would impact the SST variability in both the basins. In the BoB, the near-surface salinity stratification, in association with the precipitation from the atmosphere and riverine freshwater influx, inhibit vertical mixing process and would contribute to the increased SST (Shenoi et al., 2002, Murty et al., 2004).

The time series of NCEP/NCAR surface net heat flux and TropFlux surface net heat flux show different patterns, as reported by Praveen Kumar et al. (2013). The NCEP/NCAR net heat flux variation is similar in both AS and BoB with the epochs of net heat gain/loss across the air-sea interface. However, the long-term trend shows net heat gain over both the basins. However, the recent TropFlux air-sea heat fluxes climatology shows only net heat gain throughout the 1979-2011 period in both the AS and BoB, with relatively higher heat gain in the AS than in the BoB. The observed upward trend in the net heat gain in both the AS and BoB, particularly during 1995-2010, leads to increase in SSTs. The net heat gain during this period (1995-2010) has resulted from the observed decreasing trend in the latent heat fluxes in the same period. This upward trend in SST is also aided by the weaker contribution of horizontal advective processes during 1990-2011 in both the AS and the BoB.

It is interesting to note that the BoB exhibits higher SSTs than the AS in all the time series data products. However, over all the SST anomalies are more or less the same in both the basins. Both the time series of SST and SST anomalies show gradual increasing trend over the past few decades (1970-2010), and the SST anomaly variations are in phase in both the AS and BoB throughout the time series period. This clearly indicates that both the AS and BoB basins responded similarly to the climatic events with a warming trend, but the responses are modulated by the air-sea interaction and oceanic processes.

It is also noticed that the peaks of SST anomalies over the study period 1880-2011 are associated with the occurrences of climatic events such as the El Niño, La Niña, and the positive and negative IOD. During 1960-2008, there were 29 years where such events occurred and 19 years where no events occurred (Table 1). The seasonal SST cycle in both the AS and BoB shows seasonal warming during April-May and cooling during the peak southwest monsoon (August-September). The seasonal cycle of SST anomaly also has a seasonal cycle similar to that of SST. It is noticed that during the climatic events, the peak temperature of the seasonal cycle of SST in the AS gets modulated to a relatively higher value during April-May and lower value during August-September, when the positive IOD and El Niño events co-occurred. In the BoB, the response is delayed to November – December with relatively warmer anomalies. The response of the AS and BoB to the independent and individual climatic events is found to be weaker. In 1991, when only El Niño event occurred, the seasonal SST anomaly variation (April-September) is  $0.083^{\circ}\text{C}$  in both the AS and BoB, and in 1992, when only negative IOD event occurred, the seasonal SST anomaly variation is close to  $0.06^{\circ}\text{C}$  in the AS and BoB. It is also noticed that warmer SST anomalies in both the AS and BoB are associated with El Niño and positive IOD events and colder SST anomalies with La Niña and negative IOD events.

The long-term SST trend shows a weaker increase from 1920 and a drastic increase from 1965 onwards. The observed trends in the SST could be linked to the patterns of global observations (Morner, 1993; GISS, 2010). For this we have examined the long-term available SODA reanalysis Sea Surface Salinity (SSS) data during 1940-2008 and SSS anomalies over the long-term mean value of this period (Fig. 22a). We have also examined the available P-E (Precipitation minus Evaporation) data in the boxes of the AS and BoB (Fig. 22b). It is interesting to note that the SSS anomalies in the AS are overall steady throughout 1940-2008, whereas the BoB SSS shows an increasing trend (salting) during 1940-1972 and a decreasing trend (freshening) during 1973-2008. Positive (negative) SSS anomalies suppress (enhance) the near-surface salinity stratification, leading to enhanced (suppressed) vertical mixing processes. The long-term P-E variation (Fig. 22b) also supports the decreasing trend in the SSS in the BoB during 1980-2008. The positive SSS anomalies are due to vertical mixing in association with the lesser salinity stratification in the upper layers and, thus contributed to the negative SST anomalies. In contrast, the negative SSS anomalies lead to stronger salinity stratification in the upper layers and in turn inhibit vertical mixing, thus contributing to the positive SST anomalies and the intense surface warming. The impact of variation of stratification is more pronounced in the BoB SST variability than AS. This variation in the BoB SSS explains the negative SST anomalies during 1940-1972 and large positive SST anomalies during 1973-2008. Increased emissions of post industrial revolution and the Asian Brown Cloud (ABC) also might have contributed to a large extent to the observed trend and behaviour in SST as out in the present study. It will be interesting to examine the present results with satellite derived Sea Surface Salinity from ESA Soil Moisture and Ocean Salinity (SMOS) and NASA Aquarius missions to find answers for several of the anomalous climate state over the tropical Indian Ocean with a lead to global climate change.

## Acknowledgements

The authors thank Dr. S.W.A. Naqvi, Director, CSIR-National Institute of Oceanography, India, for providing encouragement and support. We thank Prof. Ramola Antao, consultant, Senior Cambridge English examinations in India, for editing the manuscript. This has the CSIR-NIO contribution number xxxxx.

## References

- Colborn, J.G., 1975. The upper layer thermal structure of the Indian Ocean. International Indian Ocean Expedition Monograph No. 2, Honolulu, East-West Central Press, University of Hawaii, p. 173.
- Conkright, M.E., Levitus, S., Boyer, T.P., Bartolacci, D.M., Luther, M.E., 1994. Atlas of the Northern Indian Ocean. University of South Florida, St. Petersburg, FL, 150 pp.
- Dietrich, G., 1973. The unique situation in the environment of the Indian Ocean. In: Zeitzchef, B. (Ed.), The Biology of the Indian Ocean. Springer, Berlin, pp 1-6.
- Ebenezer S. Nyadjro., Subrahmanyam, B., Murty, V.S.N., Shriver, J.F., 2012. The role of salinity on the dynamics of the Arabian Sea mini-warm pool. *J. Geophys. Res.*, 117, C09002, doi:10.1029/2012JC007978, 1-12 pp.
- Ellis, R.S., 1952. A preliminary study of a relation between surface temperature of the north Indian Ocean and precipitation over India. MS Thesis, Dept. of Meteorology, Florida State University, US.
- Felton Clifford S., Subrahmanyam, B., Murty, V.S.N., 2013. ENSO modulated cyclogenesis over the Bay of Bengal. *J. Clim.*, 26, 9806-9818, doi:10.1175/JCLI-D-13-00134.1
- Giese, B. S., Ray, S., 2011. El Niño variability in simple ocean data assimilation (SODA), 1871–2008. *J. Geophys. Res.*, 116, C02024, doi:10.1029/2010JC006695.
- Carton, J. A., Giese, B.S., 2008. A reanalysis of ocean climate using simple ocean data assimilation (SODA). *Mon. Weather Rev.*, 136, 2999–3017, doi:10.1175/2007MWR 1978.1.
- GISS, 2010. Global Land Ocean Temperature Index 1880-2010. Enter Id: GISS-12 Month Mean Global Temperature 2010. Report of the Committee on Earth Observation Satellites, USA.
- Joseph, P.V., 1990. Warm pool over the Indian Ocean and monsoon onset. *Trop. Ocean Atmos. Newslet.*, 53, 1 – 5.
- Ihara, Chie., Kushnir Yochanan., Cane A Mark., 2008. Warming Trend of the Indian Ocean SST and Indian Ocean Dipole from 1880 to 2004. *Am. Meteorol. Soc.*, 21, 2035-2046.
- Li, T., Zhang, Y., Chang, C.P., Wang, B., 2001. On the relationship between Indian Ocean surface temperature and Asian summer monsoon. *Geophys. Res. Lett.*, 28, 2843-2846.
- Molinari, R. L., Swallow, J., Festa, J.F., 1986. Evolution of the near surface thermal structure in the western Indian Ocean during FGG, 1979. *J. Mar. Res.*, 44, 739-762.
- Morner, N.A., 1992. Global sea level in the past and future century. *Bull. INQUA Neotectonics Comm.*, 16, 64-66.
- Murtugudde, R., Richard S., Prasad Thoppil., 2007. Arabian Sea response to monsoon variations. *Paleoceanography*, 22, pp4217, doi:10.1029/2007pa001467.

- Murty, V.S.N., Sarma, Y.V.B., Rao, D.P., Murty, C.S., 1992. Water characteristics, mixing and circulation in the Bay of Bengal during southwest monsoon. *J. Mar. Res.*, 50, 2, 207-228.
- Murty, V.S.N., Subrahmanyam, B., Tilvi, V., O'Brien, J.J., 2004. A new technique for the estimation of sea surface salinity in the tropical Indian Ocean from OLR. *J. Geophys. Res.*, 109, C12006, doi: 10.1029.2003JC001928.
- Nyadjro, E.S., Subrahmanyam, B., Giese, B.S., 2013. Variability of salt flux in the Indian Ocean during 1960-2008. *Remote Sensing Environ.*, 134, 175-193.
- Prasanna Kumar, S., Narvekar, J., Kumar, A., Shaji, C., Anand, P., Sabu, P., G. Rejomon, G., Josia, J., Jayaraj, K.A., Radhika, A., Nair, K.K.C., 2004. Intrusion of the Bay of Bengal water into the Arabian Sea during winter monsoon and associated chemical and biological response. *Geophys. Res. Lett.*, 31, 15, 4 pp.
- Prasanna Kumar, S., Roshin Raj P., Narvekar, J., Dinesh Kumar, P.K., Vivekanandan, E., 2009. Response of the Arabian Sea to global warming and associated regional climate shift. *Marine Environ. Res.*, 68, 5, 217-222.
- Praveen Kumar, B., Vialard, J., Lengaigne, M., Murty, V.S.N., McPhaden, M.J., 2012a. TropFlux: Air-sea fluxes for the global tropical oceans – description and evaluation. *Clim. Dyn.*, 38, 1521-1543, doi: 10.1007/s00382-011-1115.
- Praveen Kumar, B., Vialard, J., Lengaigne, M., Murty, V.S.N., McPhaden, M.J., Cronin, M.F., Gopala Reddy, K., 2012b. Evaluation of Air-sea heat and momentum fluxes for the tropical oceans and introduction of TropFlux. *CLIVAR Exchanges*, 58, 17(1), 21-24.
- Praveen Kumar, B., 2013. A study on Air-sea interactions over the tropical oceans with special emphasis on the Indian Ocean. PhD thesis, 165 pp., Andhra University, Visakhapatnam. Unpublished.
- Rao, R.R., 1988. Seasonal heat budget estimates of the upper layers in the central Arabian Sea. *Mausam*, 39, 3, 241-248.
- Rao, R.R., Kumar, P.V.H., Mathew, B., 1994. Near-surface heating in the Arabian Sea during the pre-onset regime of MONEX-79. *Meteorol. Atmos. Phys.*, 53, 19-31.
- Rao, R.R., Sivakumar, R., 1999. On the possible mechanisms of the evolution of a mini-warm pool during the pre-summer monsoon season and the genesis of onset vortex in the south-eastern Arabian Sea. *Q. J. R. Meteorol. Soc.*, 125, 787-809.
- Ramesh Babu, V., Sastry, J.S., 1984. Summer cooling in the east central Arabian sea A process of dynamic response to the southwest monsoon. *Mausam*, 35, 1, 17-26.
- Rayner, N. A., Parker, D.E., Horton, E.B., Folland, C.K., Alexander, L.V., Rowell, D.P., Kent, E.C., Kaplan, A., 2003. Global analyses of sea surface temperature, sea ice, and night marine air temperature since the late nineteenth century. *J. Geophys. Res.*, 108, D14, 4407 10.1029/2002JD002670.
- Saji, N.H., Goswami, B.N., Vinayachandran, P.N., Yamagata, T., 1999. A dipole mode in the tropical Indian Ocean. *Nature*, 401, 360-363.



Sanilkumar, V., Sajeev Philip,C., 2010. Variations in long term wind speed during different decades in Arabian Sea and Bay of Bengal. *J. Earth Sys. Sci.*, 110, 5, 639-653.

Shankar, D., Aparna, S.G., McCreary, J.P., Suresh,I., Neetu, S., Durand, F., S.S.C. Shenoi,S.S.C., Al Saafani, M.A., 2010. Minima of interannual sea-level variability in the Indian Ocean. *Progr. Oceanogr.*, 84, 225–241.

Shenoi, S. S. C., Shankar,D., Shetye,S.R., 2002. Differences in heat budgets of the near- surface Arabian Sea and Bay of Bengal: Implications for the summer monsoon. *J. Geophys. Res.*, 107, C6, 3052, doi:10.1029/2000jc000679.

Shukla, J., Misra,M., 1977. Relationship between sea surface temperature and wind speed over the central Arabian Sea and monsoon rainfall over India. *Mon. Weather Rev.*, 105, 998-1002.

Smith Thomas M., Reynolds Richard W., Thomas C Peterson, Lawrimore, J., 2008. Improvements to NOAA's Historical Merged Land–Ocean Surface Temperature Analysis (1880–2006). *J. Climate*, 21, 2283-2296, doi: 10.1175/2007JCLI2100.1.

Terray, P., 1994. An evaluation of climatological data in the Indian Ocean area. *J. Meteor.Soc. Japan*, 72, 359–386.

Terray, P., S. Dominiak., 2005. Indian Ocean sea surface temperature and El Niño–Southern Oscillation: A new perspective. *J. Climate*, 18, 1351–1368.

Torrence, C., Compo,G.P., 1998. A practical guide to wavelet analysis. *Bull. Am. Meteorol. Soc.*, 79, 61–78.

Vinayachandran, P. N., 2004. Summer cooling of the Arabian Sea during contrasting monsoons. *Geophys. Res. Lett.*, 31, L13306, doi:10.1029/2004GL019961.

Vinayachandran, P. N., Shankar, D., Kurian, J., Durand, F., Shenoi,S.S.C., 2007. Arabian Sea mini-warm pool and the monsoon onset vortex. *Current Sci.*, Special section: Indian Monsoon, 93, 2, 203-214.

Varkey, M.J., Murty, V.S.N., Suryanarayana,A., 1996. *Physical Oceanography of the Bay of Bengal and Andaman Sea. Oceanogr. Marine Biol.: an Annual Rev.*, 34, 1–70, A.D. Ansel, R. N. Gibson and Margaret Barnes (Eds.), UCL Press.

Wilson-Diaz, D., Mariano, A.J., Evans,R.H., 2009. On the heat budget of the Arabian Sea. *Deep-Sea Res. I*, 56, 141–165.

Yu, L., Weller,R.A., 2007. Objectively Analyzed air-sea heat Fluxes (OAFlux) for the global oceans. *Bull. Am. Meteor. Soc.*, 88, 527-539.

Figures:

Fig. 1. Study area showing the boxes of investigation in the Arabian Sea (AS) and Bay of Bengal (BoB).

Fig. 2. Long term ERSST Sea Surface Temperature (SST, °C) variation over the period 1880-2010 in the Arabian Sea (black curve) and the Bay of Bengal (red curve).

Fig. 3. The wavelet power spectrum for the AS for the time period from 1880 to 2010. The thick black line is the 95% significance line. The red colour outside the 95% significance line is not predominant.

Fig. 4. The wavelet power spectrum for the BoB for the time period from 1880 to 2010. The thick black line is the 95% significance line. The red colour outside the 95% significance line is not predominant.

Fig. 5. Mean seasonal cycles of ERSST Sea Surface Temperature (SST, °C) over the period 1880-2010 for the AS (black curve) and BoB (red curve).

Fig. 6. Mean seasonal cycles of ERSST SST anomaly (°C) over the period 1970-2008 (after removing the mean seasonal cycle of SST over the period 1970-2008) for the AS (black curve) box and BoB (red curve) box.

Fig. 7. ERSST SST anomalies (°C) for the period 1880-2010 (after removing the mean seasonal cycle for the period 1880-2010) in the AS (black curve) and BoB (red curve).

Fig. 8. HadleyISST SST anomalies (°C) for the period 1880-2008 (after removing the mean seasonal cycle for the period 1880-2008) in the AS (black curve) and BoB (red curve).

Fig. 9. Long term variation of Simple Ocean Data Assimilation (SODA) product SST anomalies (°C) for the period 1940-2008 (after removing the mean seasonal cycle for the period 1940-2008) in the AS (black curve) and BoB (red curve).

Fig. 10. Long term variation of TropFlux data product on SST anomalies (°C) for the period 1979-2010 (after removing the mean seasonal cycle for the period 1979-2010) in the AS (black curve) and BoB (red curve).

Fig. 11. Annual variation of ERSST anomalies (°C) (after removing the mean seasonal cycle for the period 1979-2010) during 1981-82 in the AS (blue curve) and BoB (red curve).

Fig. 12. Annual variation of ERSST anomalies (°C) (after removing the mean seasonal cycle for the period 1979-2010) during 1991-92 in the AS (blue curve) and BoB (red curve).

Fig. 13. Long term variation of monthly NCEP data product on wind speed ( $\text{m.s}^{-1}$ ) in the AS (black curve) and the BoB (red curve) during 1940-2011.

Fig. 14. Long term variation of monthly NCEP data product on shortwave radiation ( $\text{W.m}^{-2}$ ) in the AS (black curve) and BoB (red curve).

Fig. 15. Long term time series of differences in short wave radiation in the AS and BoB during 1949-2011.

Fig. 16. Long term variation of monthly TropFlux data product on short wave radiation ( $\text{W.m}^{-2}$ ) in the AS (black curve) and BoB (red curve) for the period 1979-2010.

Fig. 17. Long term variation of monthly NCEP product on total cloud cover (in percentage) in the AS (black curve) and the BoB (red curve) during 1940-2011.

Fig. 18. Long term variation of monthly NCEP product on Latent heat flux ( $\text{W.m}^{-2}$ ) in the AS (black curve) and the BoB (red curve) during 1940-2011.

Fig. 19. Long term variation of monthly NCEP product on net surface heat flux ( $\text{W.m}^{-2}$ ) in the AS (black curve) and the BoB (red curve) during 1940-2011.

Fig. 20. Long term variation of monthly TropFlux product on net surface heat flux ( $\text{W.m}^{-2}$ ) in the AS (black curve) and the BoB (red curve) during 1979-2010.

Fig. 21. Long term variation of monthly GFDL model simulated surface current speed ( $\text{m.s}^{-1}$ ) in the AS (black curve) and BoB (red curve) during 1965-2004.

Fig. 22. Long term variation of (a) SODA Sea Surface Salinity (SSS) anomalies in the AS (black curve) and BoB (red curve) for the period 1940-2008 and (b) TropFlux product of P-E anomalies for AS (black curve) and BoB (red curve) for the period 1979-2008.

## Highlights

- Examined the long-term variability of Sea Surface Temperature (SST) in the Arabian Sea (AS) and Bay of Bengal (BoB) during 1880-2010 by utilizing all the available gridded data sets.
- SST time series reveal a clear upward (increasing) trend with relatively higher values in the BoB than in the AS. However, the anomalies are found to be more or less the same.
- Delineated the major processes led to the warmer SSTs in the BoB as compared to AS.
- SST is found controlled by semi-annual and annual forcing in AS while it is influenced predominantly by annual forcing in BoB.
- The SST responses are in phase in both the basins to the climatic events such as El Niño, La Niña and Indian Ocean Dipole, but stronger impacts are noticed in the AS.

Table 1. Years of co-occurrences of IOD and ENSO events, independently occurred ENSO events and IOD events during 1960-2008 (Source: Nyadjro et al., 2013)

Co-occurrence of +ve IOD and El Niño events	Co-occurrence of -ve IOD and La Niña events	Co-occurrence of +ve IOD and La Niña events	Only -ve IOD events	Only El Niño event	Only La Niña event	No events of IOD or ENSO
1963 1972 1982 1994 1997  2006	1964 1975 1984 1989	      2007	  1992 1996  2005	1965 1968 1977 1986 1987 1991 2002	  1970 1971 1973 1974 1978 1988 1998	1960, 1962 1966, 1969 1976, 1979 1980, 1981 1983, 1985 1990, 1993 1995, 1999 2000, 2001 2003, 2004 2008
<b>6</b>	<b>5</b>	<b>1</b>	<b>3</b>	<b>7</b>	<b>7</b>	<b>19</b>

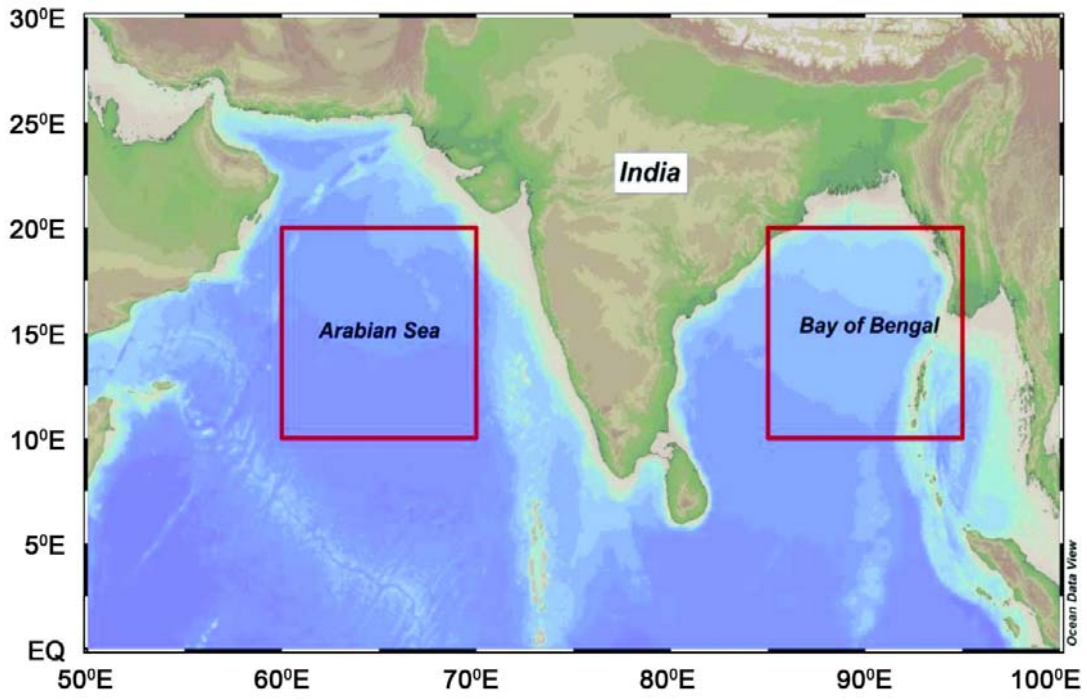


Fig.1

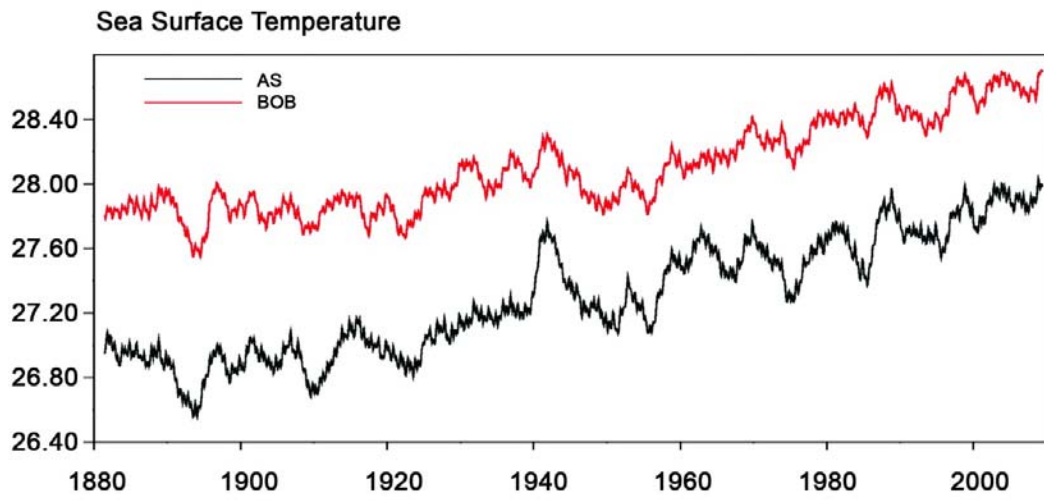


Fig. 2

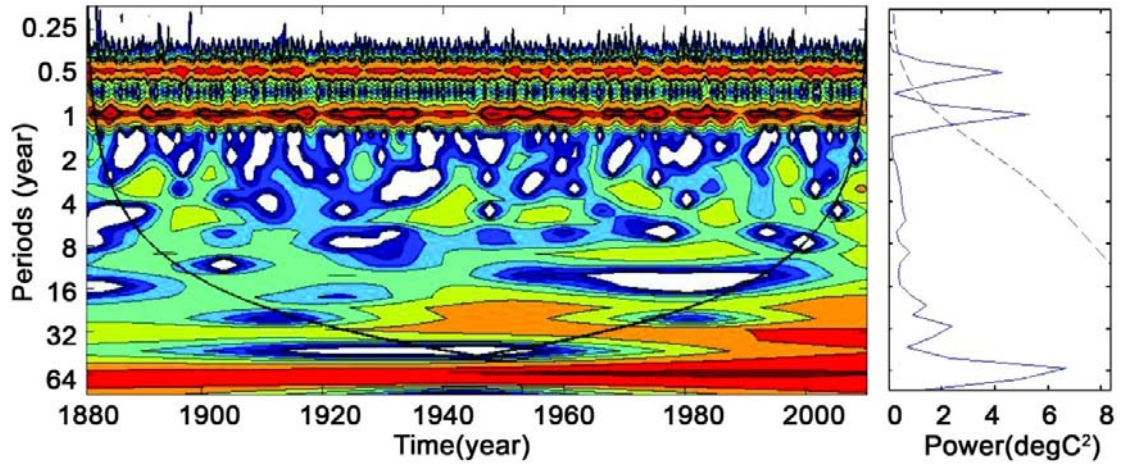


Fig. 3

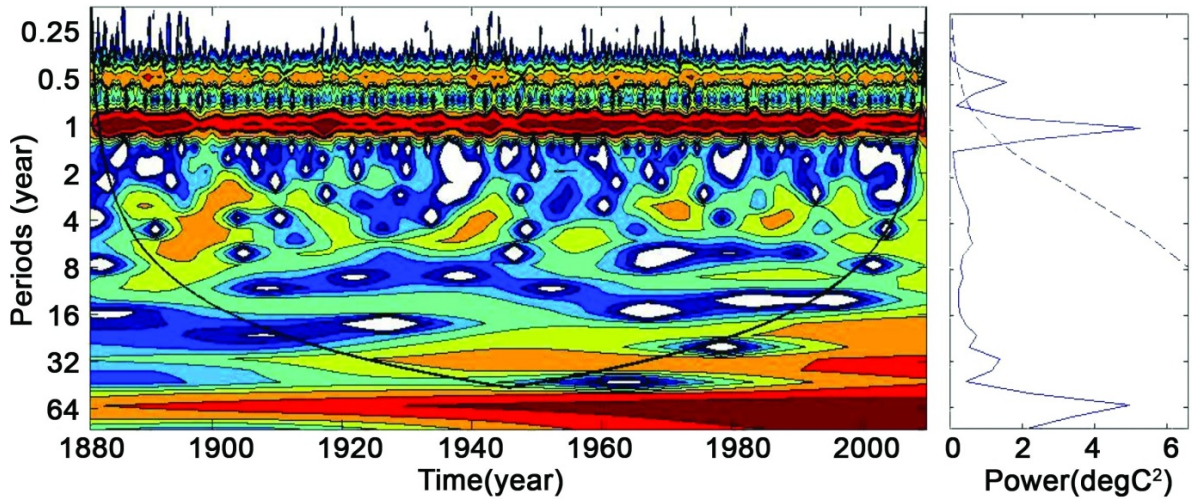


Fig. 4

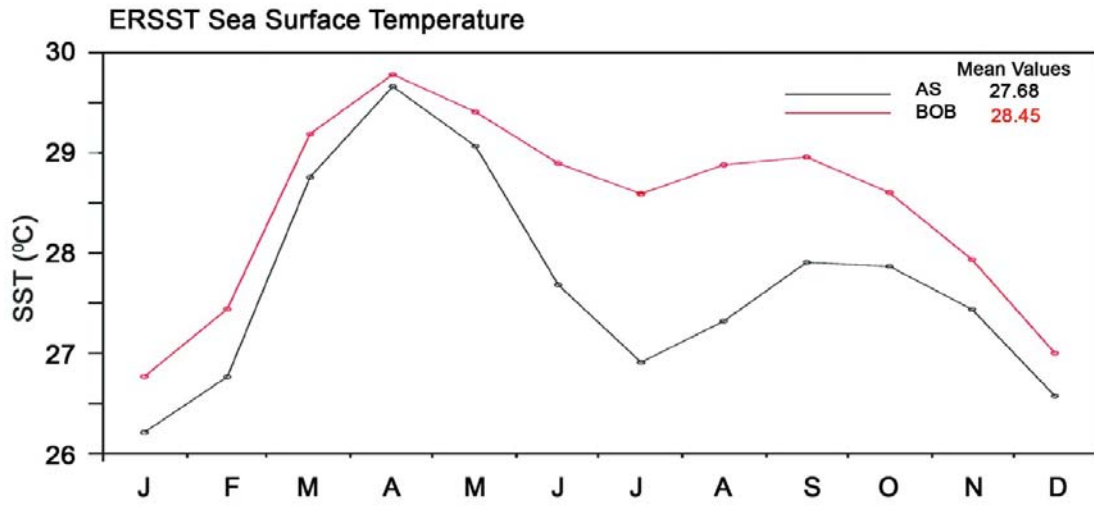


Fig. 5

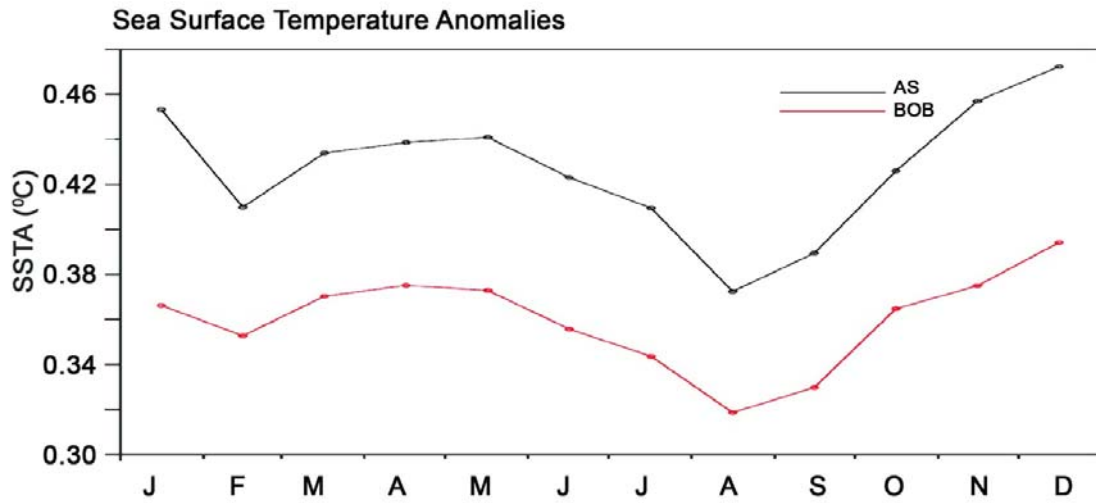


Fig.6

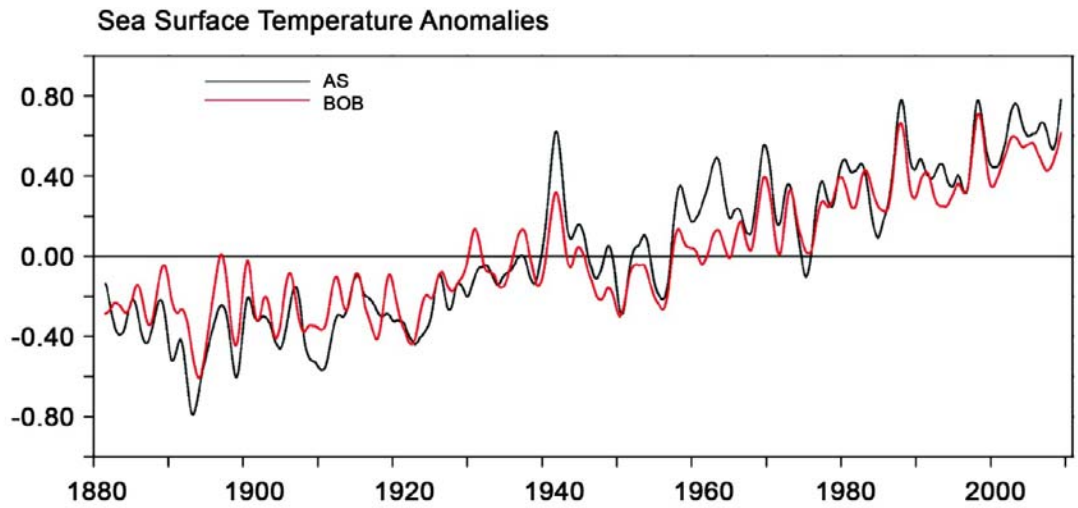


Fig. 7

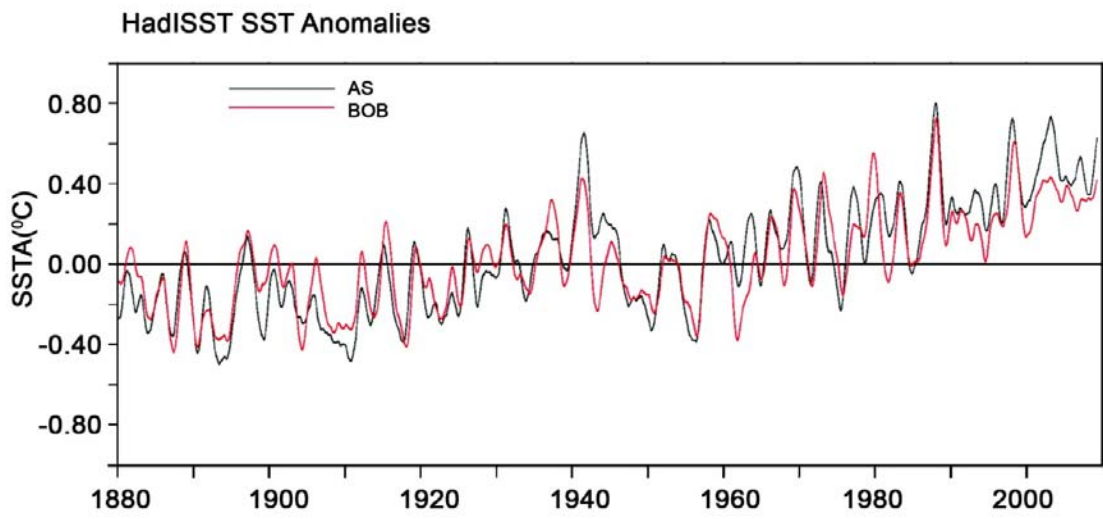


Fig. 8



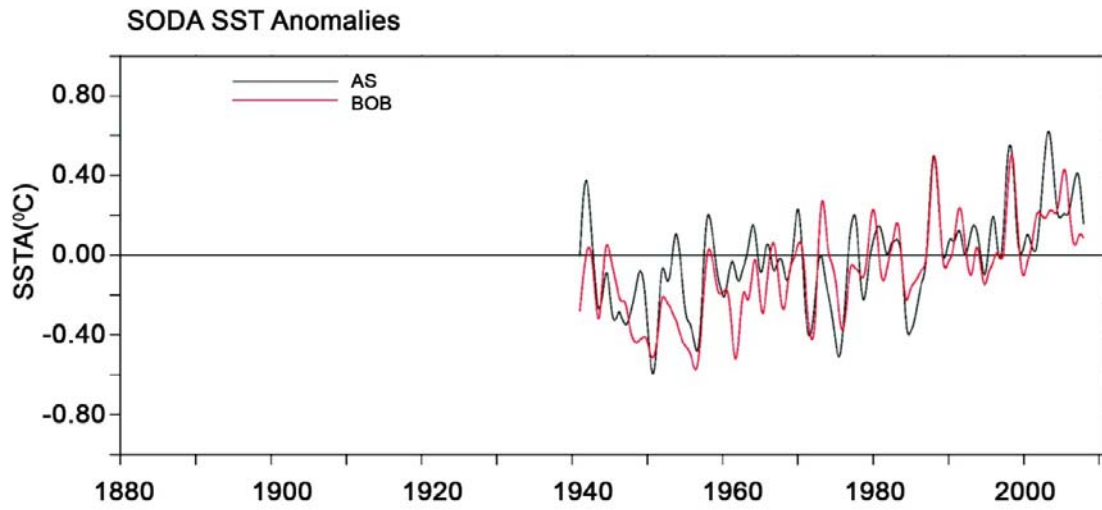


Fig.9

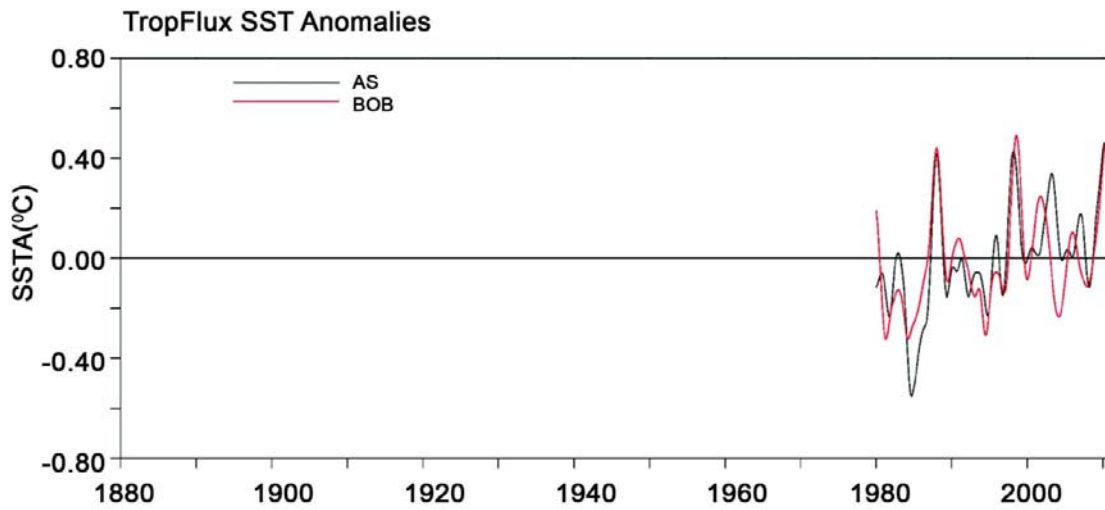


Fig. 10

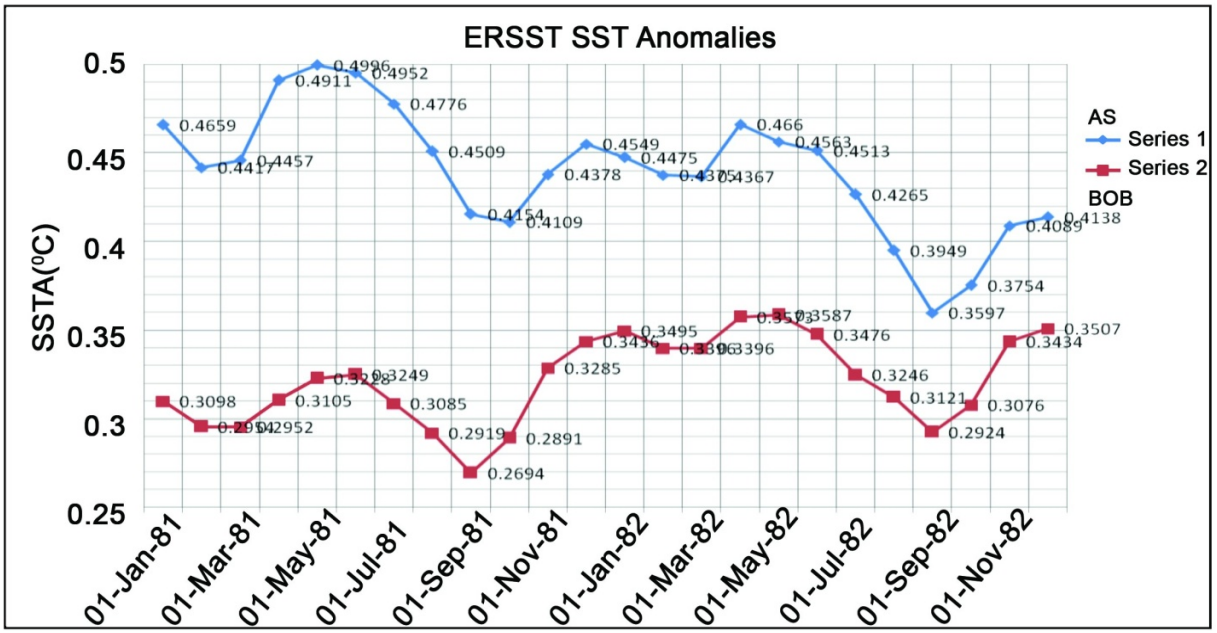


Fig.11

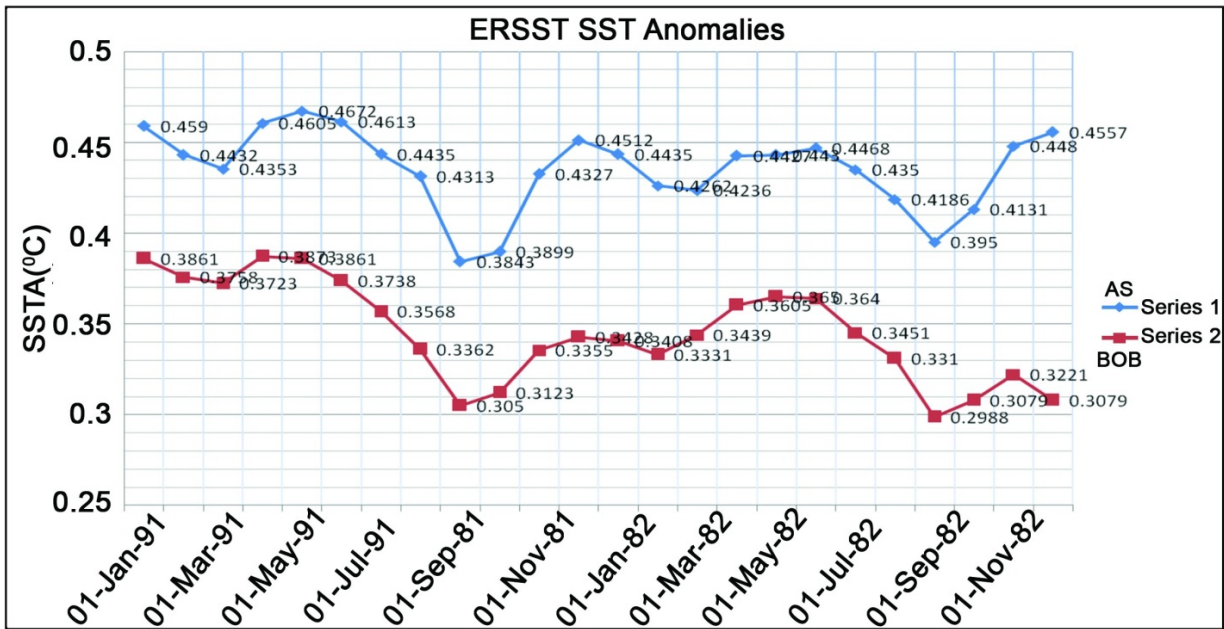


Fig. 12

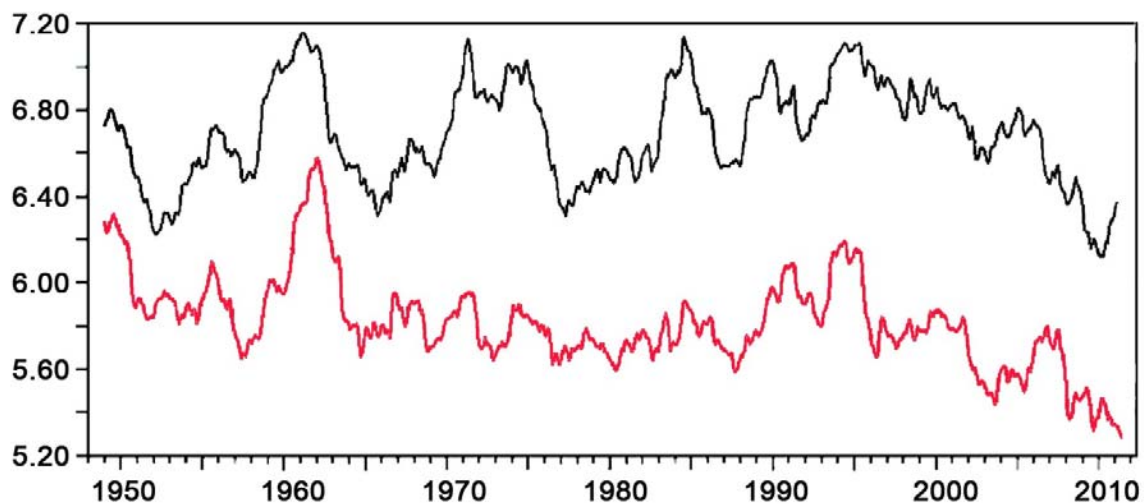


Fig. 13

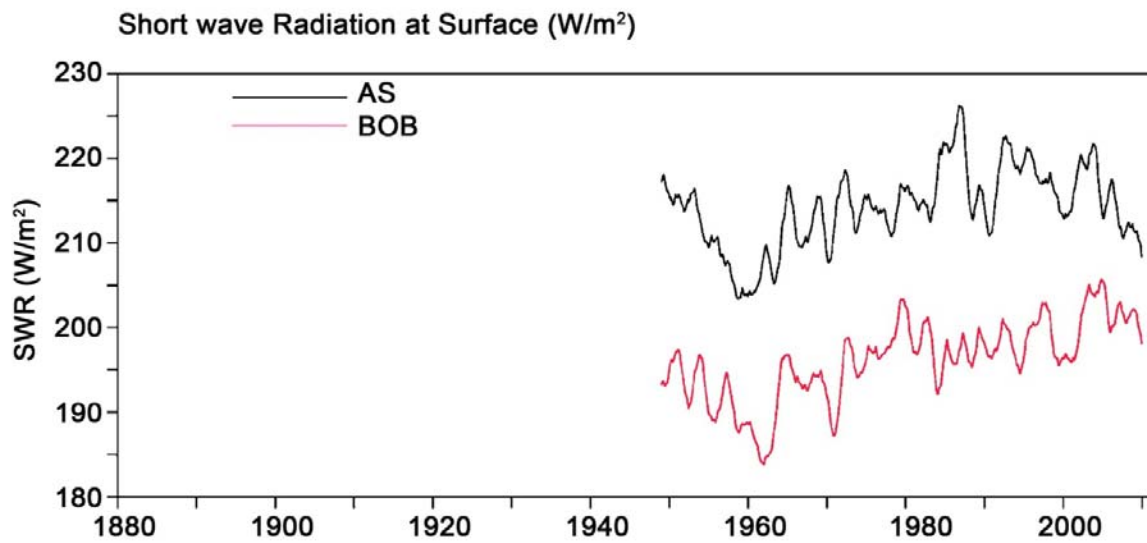


Fig. 14

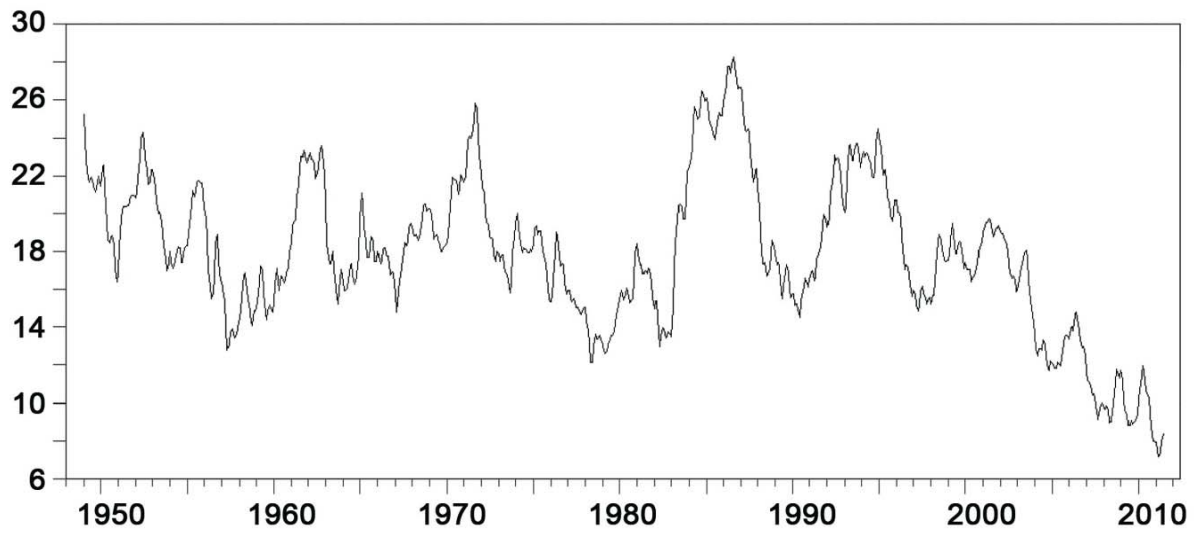


Fig. 15

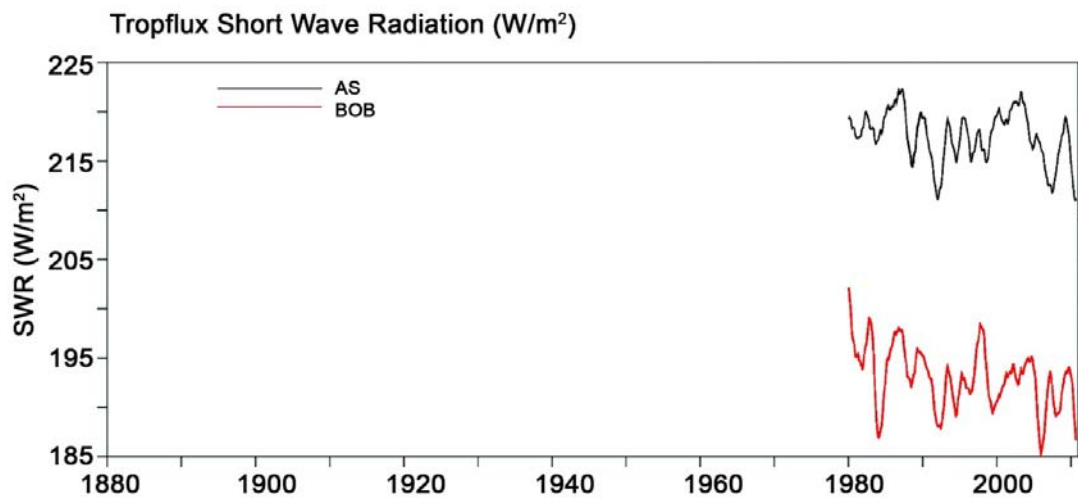


Fig.16

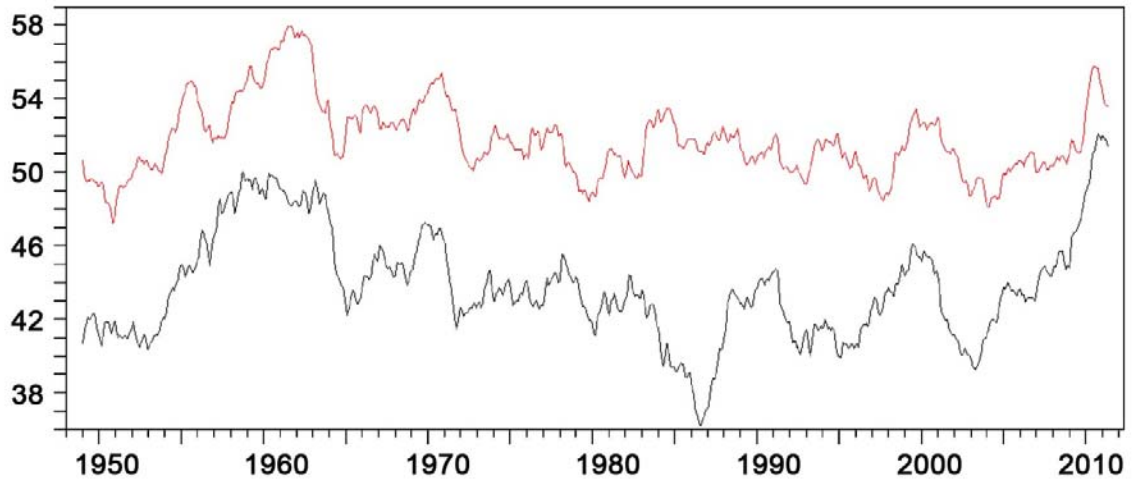


Fig.17

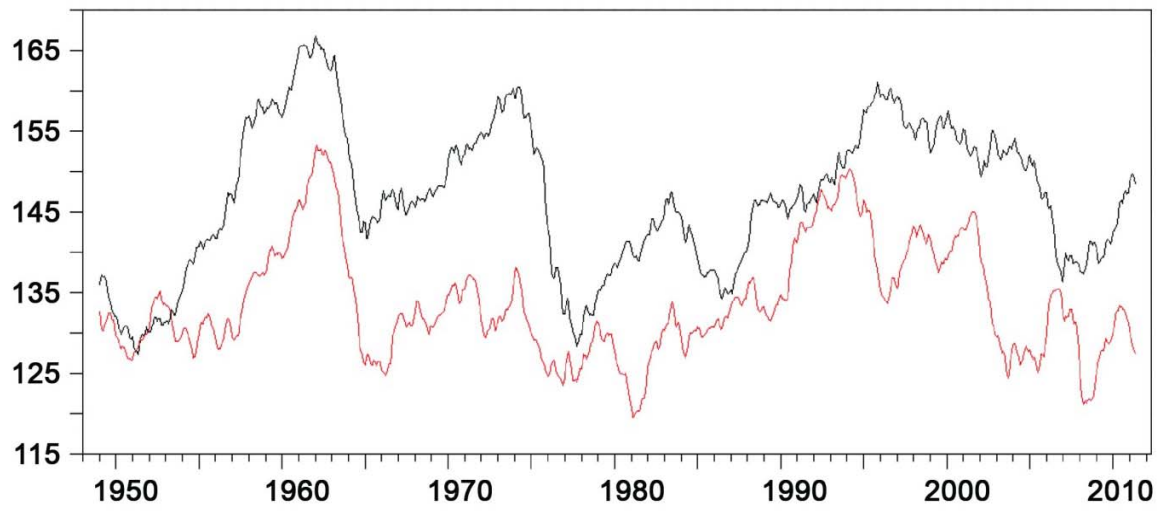


Fig.18

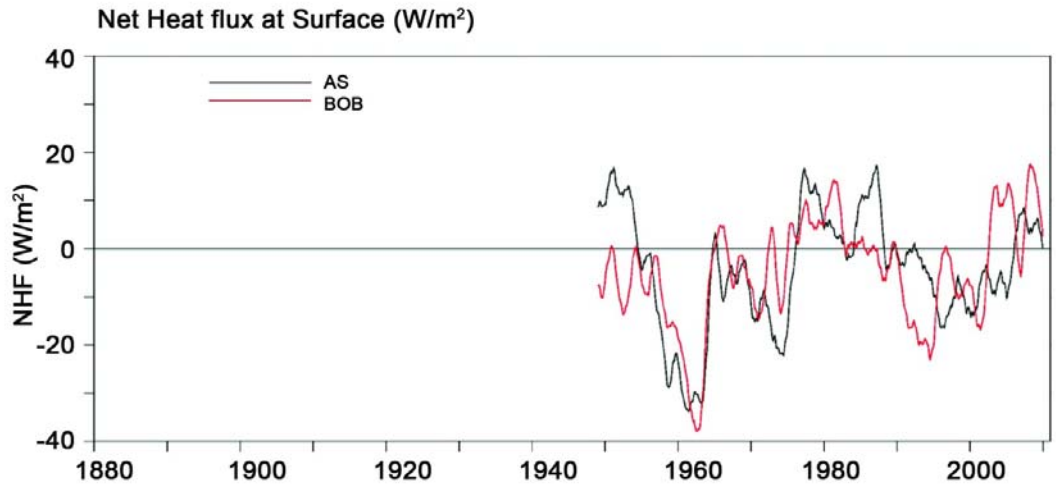


Fig.19

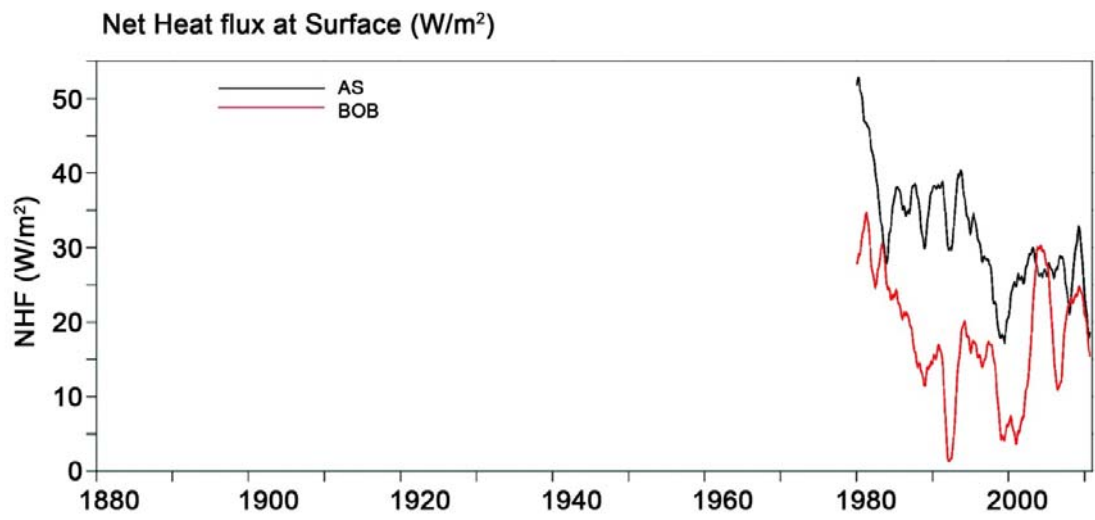


Fig. 20

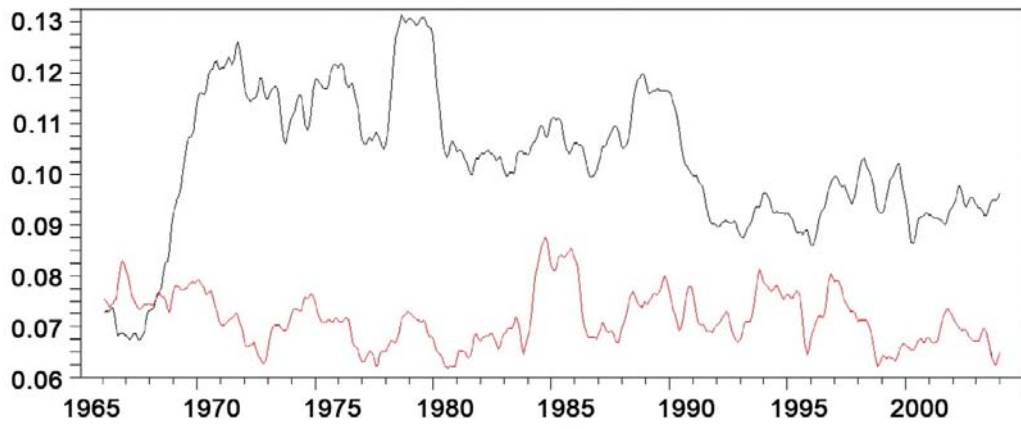


Fig.21

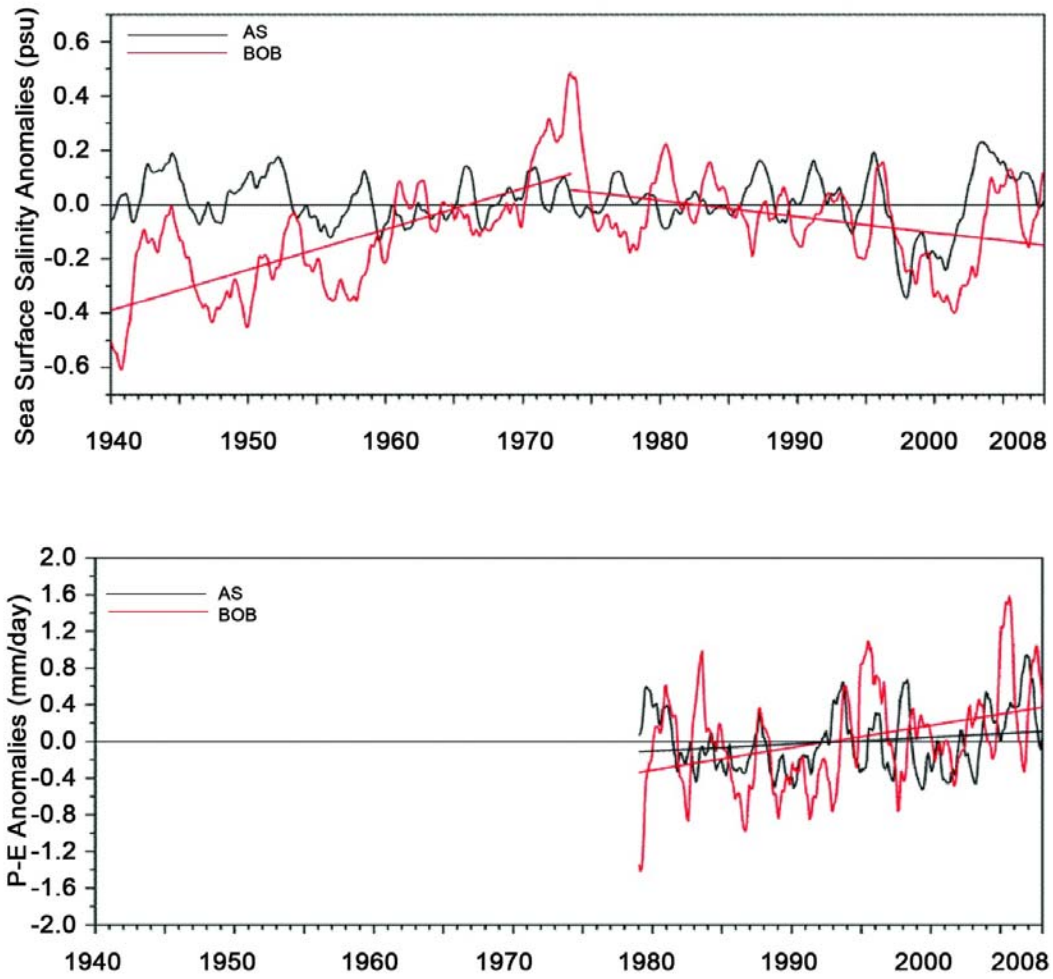


Fig. 22